engineering proceedings

MDPI

Proceeding Paper

Co-Simulation of Power Flow, Fault Behaviour, and Protection Performance Using an Integrated MATLAB–DIgSILENT Framework on IEEE Benchmark Systems †

Abuyile Mpaka * and **Senthil Krishnamurthy**

Center for Intelligent Systems and Emerging Technologies, Department of Electrical, Electronic, and Computer Engineering, Cape Peninsula University of Technology, Bellville, Cape Town 7535, South Africa; krishnamurthys@cput.ac.za
* Correspondence: ampaka4@gmail.com; Tel.: +27-787481197

† Presented at the 34th Southern African Universities Power Engineering Conference (SAUPEC 2026), Durban, South Africa, 30 June–1 July 2026.

Abstract

This study applies a combined load flow, short-circuit, and protection study of the IEEE four-bus and five-bus benchmarks as a comprehensive approach to power system modelling. A consistent per-unit base of 150 MVA and 132 kV is applied uniformly. The NR co-simulation approach is used for load flow studies in both MATLAB_R2025b and DIgSILENT PowerFactory 2025. The simulation results indicate that voltages, power mismatches, and line flows are within the tolerance limits. Findings suggest that the NR method was highly implementable, yielding results in 2–3 iterations, and that the simulation results were comparable to those produced by commercial software, validating confidence in the power system modelling, load flow analysis, and protection study.

Keywords: residential Newton–Raphson; load flow; DIgSILENT; MATLAB; short-circuit; overcurrent protection; IEEE test systems

Academic Editor: Akshay Kumar Saha

Published: 12 May 2026

1. Introduction

Today's electrical power systems are increasingly complex due to rising demand, interconnected systems, and the integration of renewable resources. Reliable systems can operate effectively if steady-state and fault-level conditions are understood; load flow and short-circuit analysis are standard processes in system design and operation [1–3]. Load flow analysis determines the bus voltages, phase angles, line flows, and losses in a system under normal operating conditions. The information obtained through load flow forms the basis of voltage control assessments, equipment loading, and contingency (loss allowance) [4].

The three most commonly used load flow methods are Gauss–Seidel, Fast Decoupled, and Newton–Raphson. Gauss–Seidel is relatively simple to implement and has a lower computational cost, yet it is the slowest method available. Furthermore, Gauss–Seidel may provide limited results due to its sensitivity to initial guess estimates [5]. Fast Decoupled is faster than Gauss–Seidel but less accurate on weakly or heavily loaded systems, making it the second-best method. Therefore, Newton–Raphson is the preferred algorithm for most medium- and large-scale networks because a combined approach yields higher quadratic convergence, resulting in numerical robustness not found in the other two methods—especially in all-conditioned systems [6]. Newton–Raphson load flow can be found in

https://doi.org/10.3390/engproc2026140002

commercial software like DIgSILENT PowerFactory 2025, MATLAB_R2025b, and ETAP, making it the most applicable power system study [7].

Similarly, accurate short-circuit analysis is an antecedent for protective coordination studies [8] (i.e., choosing relay inverse-time characteristics), equipment rating for operation (to avoid overload conditions) and fault ride-through assessments [9]. The IEC 60909 standard [10] provides a method for calculating the prospective fault current of three-phase AC networks. Overcurrent protective methods today depend on accurate calculations from these fault-practical standards for proper discrimination/selectivity; time–current curves are derived from precise fault calculations [11,12]. In addition, the software DIgSILENT PowerFactory 2025 and MATLAB_R2025b can both effectively generate models from input data to produce automated or analytically derived reports [13].

The analysis is both analytical and simulation-based and is performed in two parts on the IEEE four-bus and five-bus systems. In Part 1, Case 1, the four-bus system experiences Newton–Raphson load flow and an IEC 60909 three-phase fault. In Part 1, Case 2, the system is extended to a five-bus situation with additional overcurrent relay coordination. Thus, the relative analyses in each part's case are based on p.u. information on Y-bus formulation, NR load flow calculations, and symmetrical fault calculation, all compared to MATLAB_R2025b and DIgSILENT PowerFactory 2025 findings. Therefore, it is both a unified theoretical investigation and a software-based investigation of non-faulted and faulted conditions across all systems.

The paper is organised as follows. The introduction and literature summary are in Section 1. Section 2 provides the Newton–Raphson co-simulation methodology. Sections 3 and 4 present use-case studies to validate the proposed NR co-simulation results for the IEEE benchmark systems, and Section 5 discusses the simulation results and provides a conclusion.

2. Newton–Raphson Co-Simulation Methodology

Theoretical standards for reliable power system analysis are relevant to field parameterisation across the interconnected grid and to the adequate application of methods and calculations. This chapter will provide theoretical support for each corresponding case study regarding per-unit system modelling, Y-bus construction, Newton–Raphson load flow, and IEC 60909 short-circuit considerations.

2.1. Per-Unit System Modelling

Per unit (p.u.) values are voltages, currents, impedances, and powers defined as fractions of selected arbitrary base values—this represents relative measurement p.u. The system applies to all buses and transmission lines, helping maintain consistency and making system-wide testing/comparisons and equivalency assessments across vast, interconnected systems easier.

For example, the 4-bus system is based on 150 MVA and 132 kV, while the 5-bus system is based on 100 MVA and 230 kV. Thus, once per unit, it is easy to represent them back in real life with the established base values. The simulation and analysis were carried out using MATLAB_R2024a

$$Z_{actual} = Z_{pu} \cdot Z_{base}, \quad Z_{base} = \frac{V_{base}^2}{S_{base}} \tag{1}$$

This normalisation enables consistent calculation of line impedances, voltages, and currents across the network.

2.2. Y-Bus Construction

The first step of any load flow solution is the Y-bus matrix (bus admittance matrix). The Y-bus matrix is constructed by application of Kirchhoff's Current Law (KCL) to the respective buses of interest, where the admittance corresponding to the transmission lines connecting the buses of interest is summed to the shunt connected to the buses of interest. The typical equation for a bus with network buses is

$$I_i = \sum_{j=1}^{n} Y_{ij} V_j \tag{2}$$

The diagonal entries of the admittance matrix become the self-admittance of interest, and the off-diagonal entries adjacent become the negative admittance associated with the line connecting the two buses of interest. Thus, a constructed Y-bus will enable parameterisation, allowing the voltage magnitude and angle of interest to be determined via power flow.

2.3. Newton–Raphson Load Flow Equations

The Newton–Raphson (N-R) power flow technique is employed, an iterative method for resolving system nonlinear equations. NR Load Flow performs the iterations outlined in the flowchart shown in Figure 1. In other words, it makes an assumption about the voltage (initial voltage) at each bus and, based on the real (P) and reactive (Q) power mismatch equations, repeatedly adjusts each bus value until its final answer. Since the strategy linearises through the Taylor series, it can converge rather quickly. For the load buses, the P and Q mismatch equations are as follows:

$$P_i = V_i \sum_{k=1}^{n} V_k Y_{ik} \cos(\theta_{ik} - \delta_i + \delta_k)$$

$$Q_i = V_i \sum_{k=1}^{n} V_k Y_{ik} \sin(\theta_{ik} - \delta_i + \delta_k) \tag{3}$$

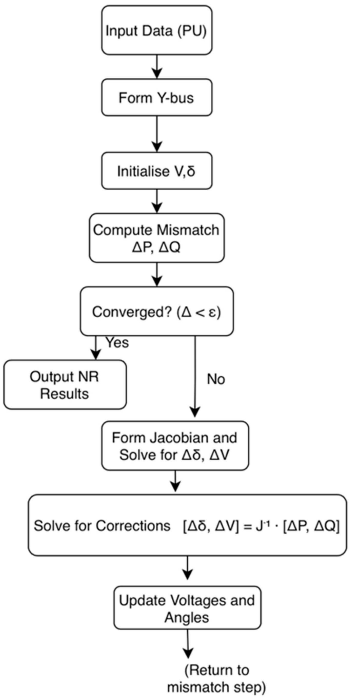

Figure 1. Newton–Raphson flow chart diagram.

The voltage corrections are obtained using the Jacobian matrix J:

$$\begin{bmatrix} \Delta\delta \\ \Delta V \end{bmatrix} = J^{-1} \begin{bmatrix} \Delta P \\ \Delta Q \end{bmatrix} \tag{4}$$

The NR algorithm solves nonlinear power flow equations using Taylor-series linearisation:

$$X^{k+1} = X^k - J^{-1} F\left(X^k\right) \tag{5}$$

The quadratic convergence of the NR method makes it highly suitable for both small- and large-scale networks.

2.3.1. Per-Unit Conversion

All system quantities are converted using a base of 150 MVA and 132 kV:

$$Z_{pu} = Z_{actual} \frac{S_{base}}{V_{base}^2} \tag{6}$$

2.3.2. Bus Injection Calculation

Before obtaining the final per-unit injections, two intermediate steps are required.
Step 1—Convert system base values.
Given $S_{base} = 150$ MVA,
Bus 2 real power generation: P_{G2} = 100 MW;
Bus 2 reactive power generation: Q_{G2} = 50 Mvar.
Step 2—Convert actual values to per-unit using

$$P_{pu} = \frac{P}{S_{base}}, \quad Q_{pu} = \frac{Q}{S_{base}} \tag{7}$$

$$P_2 = \frac{100}{150} = 0.667\ pu, \quad Q_2 = \frac{50}{150} = 0.333\ pu \tag{8}$$

2.3.3. Y-Bus Matrix Formation

Line admittances are computed from the series impedances using

$$Y_{ij} = -\frac{1}{Z_{ij}} \tag{9}$$

And diagonal elements follow

$$Y_{ij} = \sum_{j \neq i} Y_{ij} \tag{10}$$

NR solves the nonlinear power flow equations by iteratively improving estimates of voltage magnitudes and angles until the mismatch in system powers approaches zero. This is accomplished by

$$\Delta P_i = P_i^{spec} - P_i^{calc}, \ \Delta Q_i = Q_i^{spec} - Q_i^{calc}$$

$$\begin{bmatrix} \Delta\delta \\ \Delta V \end{bmatrix} = J^{-1} \begin{bmatrix} \Delta P \\ \Delta Q \end{bmatrix} \tag{11}$$

3. Case Study and Simulation Results on IEEE Four-Bus System

The effectiveness of the IEEE four-bus and five-bus systems is subjected to the methodology of Section 2. The following solutions were found: per-unit conversion, Y-bus formation, NR load flow, and IEC 60909 short-circuit. The line impedances and their corresponding admittances for Y-bus formation are located in Table 1.

Table 1. Line impedance and admittance values.

Lines Code		Resistance: R per Unit	Reactance: X per Unit
1–2	2–1	0.0100	0.0530
1–3	3–1	0.0109	0.0483
1–3	4–1	0.0120	0.0497
2–4	4–2	0.0110	0.0512
3–4	4–3	0.0125	0.0499

A. *MATLAB load flow simulation*

In Figure 2, the four-bus network is compiled for the MATLAB_R2024b load flow approach to provide further visual confirmation of system parameters. Figure 3 shows bus voltage and power flow results for the system, indicating the overall performance of bus voltages and the relationships among connections under the assumed load in steady state.

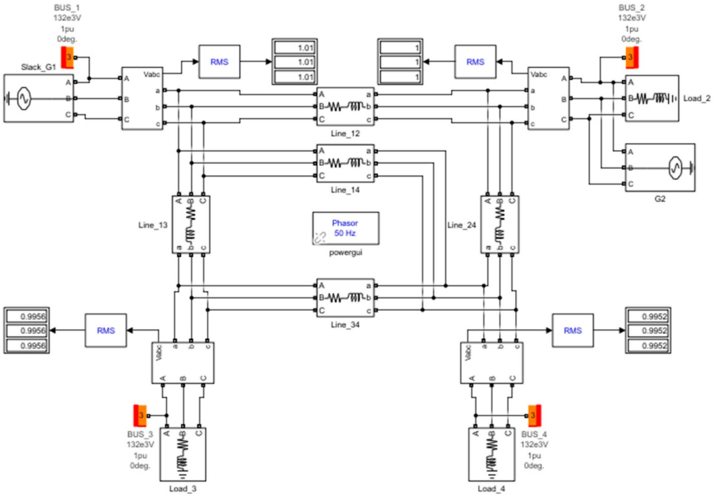

Figure 2. Four-bus network load flow in MATLAB simulation tool.

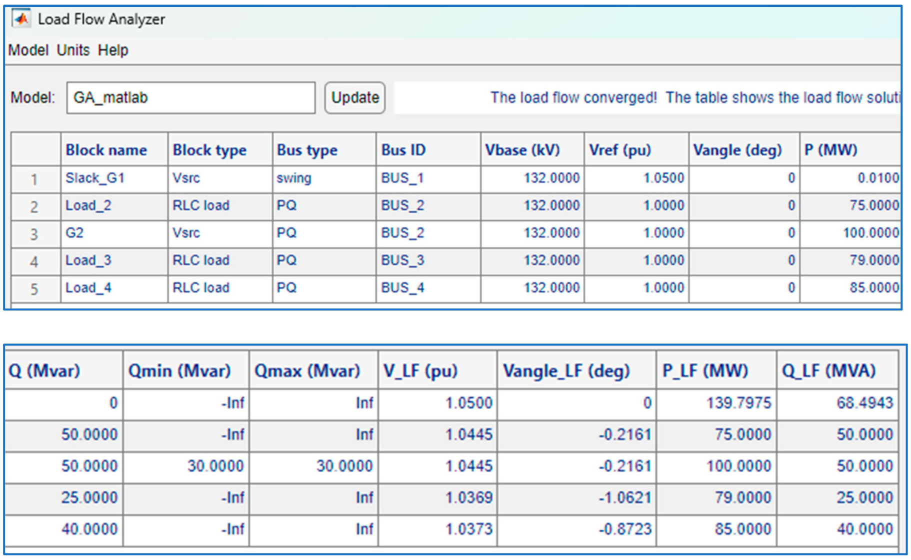

Model: GA_matlab

The load flow converged! The table shows the load flow soluti

	Block name	Block type	Bus type	Bus ID	Vbase (kV)	Vref (pu)	Vangle (deg)	P (MW)	Q (Mvar)	Qmin (Mvar)	Qmax (Mvar)	V_LF (pu)	Vangle_LF (deg)	P_LF (MW)	Q_LF (MVA)
1	Slack_G1	Vsrc	swing	BUS_1	132.0000	1.0500	0	0.0100	0	-Inf	Inf	1.0500	0	139.7975	68.4943
2	Load_2	RLC load	PQ	BUS_2	132.0000	1.0000	0	75.0000	50.0000	-Inf	Inf	1.0445	-0.2161	75.0000	50.0000
3	G2	Vsrc	PQ	BUS_2	132.0000	1.0000	0	100.0000	50.0000	30.0000	30.0000	1.0445	-0.2161	100.0000	50.0000
4	Load_3	RLC load	PQ	BUS_3	132.0000	1.0000	0	79.0000	25.0000	-Inf	Inf	1.0369	-1.0621	79.0000	25.0000
5	Load_4	RLC load	PQ	BUS_4	132.0000	1.0000	0	85.0000	40.0000	-Inf	Inf	1.0373	-0.8723	85.0000	40.0000

Figure 3. MATLAB load flow simulation results.

4. Case Study and Simulation Results on IEEE Five-Bus System

The configuration of the IEEE five-bus network used for load, fault, and protection analysis is shown in Figure 4 as the complete single-line diagram of the system.

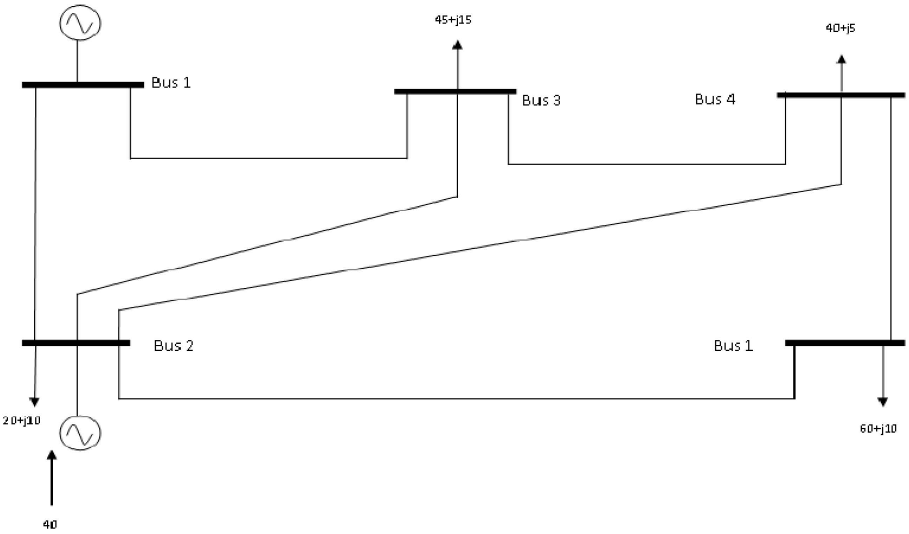

Figure 4. IEEE 5-bus single-line diagram.

4.1. Newton–Raphson Load Flow Results

The results of NR load flow for the five-bus network are compiled in Figure 5 with steady-state bus voltages, angles, and power injections provided. These results show consistent NR convergence and stability for further short-circuit and protection evaluations.

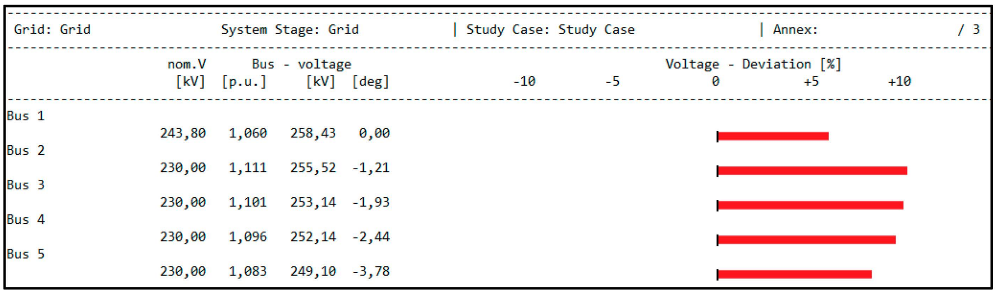

```
--------------------------------------------------------------------------------------------------------
Grid: Grid                 System Stage: Grid          | Study Case: Study Case           | Annex:          / 3
--------------------------------------------------------------------------------------------------------
                 nom.V      Bus - voltage                               Voltage - Deviation [%]
                  [kV]  [p.u.]     [kV]  [deg]          -10        -5          0          +5         +10
--------------------------------------------------------------------------------------------------------
Bus 1
                243,80   1,060   258,43   0,00
Bus 2
                230,00   1,111   255,52  -1,21
Bus 3
                230,00   1,101   253,14  -1,93
Bus 4
                230,00   1,096   252,14  -2,44
Bus 5
                230,00   1,083   249,10  -3,78
```

Figure 5. Five-bus NR load flow results.

4.2. Short-Circuit Study

For Buses 2, 3, and 5, an expected balanced three-phase fault was applied during testing in accordance with IEC 60909 standards, as evidenced by the equation below.

$$I_{sc,2} = \frac{V_n}{Z_{th}} = 5.27\ \text{kA} \tag{12}$$

This provides a total fault current consistent with the system short-circuit capacity, which has been calculated. For Buses 2, 3, and 5, a full range of expected total fault currents is provided in Table 2, with expected short-circuit levels consistent with medium-voltage systems.

Table 2. DigSilent short-circuit analysis output.

Bus No.	Bus Name/Node	Rated Volt. (kV)	Ikss (kA)	Ip (kA)	Ik"/Ipk (kA)	Ik (kA)	Uc (%)	Zth (Ω)
1	Bus_1	132.0	12.45	9.40	8.10	10.2	5.8	$0.0102\angle$-86°
2	Bus_2	33.0	6.32	4.76	4.10	5.2	7.1	$0.0208\angle$-80°
3	Bus_3	11.0	3.20	2.45	2.05	2.6	9.4	$0.0451\angle$-75°
4	Bus_4	11.0	1.18	0.90	0.75	0.95	1.8	$0.1520\angle$-70°
5	Bus_5	0.415	0.42	0.31	0.27	0.33	11.2	$0.950\angle$-60°

4.3. Overcurrent Protection

Overcurrent protection settings were theoretically calculated to discriminate between primary and backup relays, with pickup settings, TMS values, and relay operating times compiled in Figure 6 along with their appropriate time–current coordination curves, which grade appropriately between relays and are validated through adequate clearance.

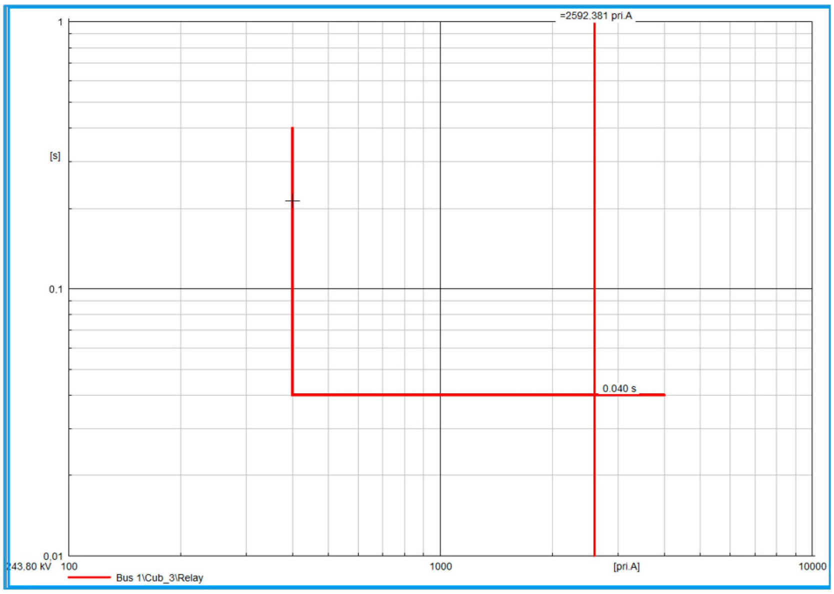

Figure 6. Time–current coordination curves, relay settings and operating times and the standard IEC inverse-time equation.

The overcurrent relay settings were derived using Equation (13)

$$I_{pickup} = 1.3 I_{load} \tag{13}$$

5. Conclusions

Overall, this project analysed an IEEE small-scale electrical network using an NR co-simulation approach for load flow analysis and extended this to symmetrical short-circuit assessment and overcurrent protection studies, providing a blended educational venture through Newton–Raphson power calculations, DigSilent Power Factory modelling, and Simscape-equivalent MATLAB options, all independently developed to validate simulation results and assess computational feasibility for successful power system modelling and assessment. Future work will consist of integrating renewable energy sources and validating the developed co-simulation approach for large-scale IEEE test systems.

Author Contributions: S.K.: conceptualisation, methodology, software, validation. A.M. and S.K.: formal analysis, investigation. S.K.: resources, data, editing, supervision, visualisation, project administration, funding acquisition. A.M. and S.K.: writing, reviewing, editing. All authors have read and agreed to the published version of the manuscript.

Funding: This work was supported in part by the National Research Foundation (NRF), under Thuthuka Grant 138177; in part by the Eskom Tertiary Education Support Program (TESP) through a research grant; and in part by the Eskom Power Plant Engineering Institute (EPPEI), French Embassy AI-Furgal Grant 2025-135.

Institutional Review Board Statement: Not applicable.

Informed Consent Statement: Not applicable.

Data Availability Statement: Data are contained within the article.

Acknowledgments: The researchers acknowledge the support and assistance of the Center for Intelligent Systems and Emerging Technologies at the Department of Electrical, Electronic, and Computer Engineering, Cape Peninsula University of Technology, Bellville, Cape Town 7535, South Africa, for their financial and material assistance in executing this research project. The opinions presented in this paper are those of the authors and not the funders.

Conflicts of Interest: The authors declare no conflicts of interest.

References

1. Li, D.; Su, Y.; Wang, F.; Olama, M.; Ollis, B.; Ferrari, M. Power Flow Models of Grid-Forming Inverters in Unbalanced Distribution Grids. *IEEE Trans. Power Syst.* **2024**, *39*, 4311–4322. [CrossRef]
2. Saha, S.; Alam, F.; Sayada, R.; Rahman, R.M.; Hasan, A.S.M.J. Advanced Load Flow & Fault Analysis of Renewable Energy Integration in IEEE 9 Bus Power System. In *IEEE Global Energy Conference 2024 (GEC 2024)*; Institute of Electrical and Electronics Engineers (IEEE): Piscataway, NJ, USA, 2024; pp. 338–347. [CrossRef]
3. Zhang, B.; Wang, M.; Su, W. Reliability Analysis of Power Systems Integrated with High-Penetration of Power Converters. *IEEE Trans. Power Syst.* **2021**, *36*, 1998–2009. [CrossRef]
4. Song, J.; Fanals-Batllori, J.; Marín, L.; Cheah-Mane, M.; Prieto-Araujo, E.; Bullich-Massagué, E.; Gomis-Bellmunt, O. A short-circuit calculation solver for power systems with power electronics converters. *Int. J. Electr. Power Energy Syst.* **2024**, *157*, 109839. [CrossRef]
5. Guevara-Velandia, G.-A.; Rairán-Antolines, J.-D. Advancements in Three-Phase Short-Circuit Fault Computation for Power System Generators: A Comprehensive Review. *Rev. Fac. Ing. Univ. Pedagog. Y Tecnol. Colomb.* **2024**, *33*, e15945. [CrossRef]
6. Park, J.; Askarian, A.; Salapaka, S. Control Designs for Critical-Contingency Responsible Grid-Following Inverters and Seamless Transitions To and From Grid-Forming Modes. Mar. 2024. Available online: http://arxiv.org/abs/2403.15380 (accessed on 1 March 2024).
7. Geng, S.; Chatterjee, S. Unified Control Scheme for Optimal Allocation of GFM and GFL Inverters in Power Networks. Dec. 2024. Available online: http://arxiv.org/abs/2412.15446 (accessed on 1 December 2024).
8. Bhowmik, B.; Acquah, M.A.; Kim, S.-Y. Hybrid compatible grid forming inverters with coordinated regulation for low inertia and mixed generation grids. *Sci. Rep.* **2025**, *15*, 29996. [CrossRef] [PubMed]
9. Nawaz, A.; Hafeez, G.; Khan, I.; Jan, K.U.; Li, H.; Khan, S.A.; Wadud, Z. An Intelligent Integrated Approach for Efficient Demand Side Management with Forecaster and Advanced Metering Infrastructure Frameworks in Smart Grid. *IEEE Access* **2020**, *8*, 132551–132581. [CrossRef]
10. *IEC 60909-0:2016*; Short-Circuit Currents in Three-Phase a.c. Systems. International Electrotechnical Commission: Geneva, Switzerland, 2016.
11. Haddadi, A.; Farantatos, E.; Patel, M.; Kocar, I. Need for Load Modeling in Short Circuit Analysis of an Inverter-Based Resource-Dominated Power System. *IEEE Trans. Power Deliv.* **2023**, *38*, 1882–1890. [CrossRef]
12. Lone, M.A.; Singh, K.A.; Singh, P. Advanced Load Flow Analysis Techniques in MATLAB the Swing Equation and Newton-Raphson Method. *Int. J. Sci. Res. Eng. Trends* **2024**, *10*, 2685–2693.
13. Strezoski, L.; Prica, M.; Loparo, K.A. Sequence Domain Calculation of Active Unbalanced Distribution Systems Affected by Complex Short Circuits. *IEEE Trans. Power Syst.* **2018**, *33*, 1891–1902. [CrossRef]

https://doi.org/10.3390/engproc2026140002